C. Padmanabhan
Graduate Research Associate.

R. C. Barlow
Graduate Research Associate.

T. E. Rook
Graduate Research Associate.

R. Singh
Professor.
Fellow ASME

Acoustics and Dynamics Laboratory,
Department of Mechanical Engineering,
The Ohio State University,
Columbus, OH 43210-1107

Computational Issues Associated with Gear Rattle Analysis

This paper proposes a new procedure for formulating the gear rattle type problem analytically before attempting a numerical solution. It also outlines appropriate evaluation criteria for direct time domain integration algorithms used to solve such problems. The procedure is necessary due to the non-analytical nature of the mathematical formulation describing vibro-impacts, which can lead to numerical "stiffness" problems. The method is essentially an "intelligent" pre-processing stage and is based on our experience in simulating such systems. Important concepts such as model order reduction, gear or clutch stiffness contact ratio, appropriate choice of non-dimensionalization parameters are illustrated through examples. Several case studies of increasing complexity are solved using various well known numerical algorithms; solutions are compared qualitatively and quantitatively using the proposed evaluation criteria, and specific numerical problems are identified. Some of the simulation models have also been validated by comparing predictions with experimental data.

1 Introduction

Gear backlash induced vibro-impacts have been studied by using a variety of techniques such as digital simulation (Sakai et al., 1981; Singh et al., 1989; Chikatani and Suehiro, 1991), analog simulation (Veluswami and Crossley, 1975; Comparin and Singh, 1990), quasi-steady state analysis (Seaman et al., 1984), multi-body approach (Pfeiffer and Kunert, 1990) and experimental noise perception (Croker et al., 1990; Johnson and Hirami, 1991). Most of the studies have focused on the rattle phenomena in automotive manual transmissions. A number of research issues still remain unresolved (Singh et al., 1989; Pfeiffer and Kunert, 1990). Numerical solutions issue, the focus of this paper, is one typical example of such research problems which are of interest both from academic and practical viewpoints.

Consider the example case of an automotive transmission. Multiple clearance nonlinearities associated with backlash between gears, multi-staged clutches or dampers, dual mass flywheel, spline or synchronizer backlash and bearing clearances are typically encountered in a given problem. Obviously, one should attempt to model the complete transmission system, however, the dimension of analysis is usually too large. Accordingly reduced order models must be pursued (Singh et al., 1989; Comparin and Singh, 1990). Several investigators have even examined only the flywheel-clutch system. Whether such a reduced order model is appropriate, it is difficult to assess *a priori*. Since the number of degrees of freedom involved is fairly large, numerical simulation of the deterministic system is often the preferred method of solution. However, some of the earlier investigations (Singh et al., 1989; Croker et al., 1990) have reported numerical difficulties in the direct time domain integration process. These are directly related to the nature of the vibro-impact model which is non-analytic. The periodic occurrence of impacts causes high frequency transients resulting in rapid reduction in step sizes. In addition, the ratio of the largest (in magnitude) to the smallest (non-zero) eigenvalue of the system matrix may become very large causing an ill-conditioning of the system matrix. These two phenomena cause the system to be characterized as "stiff" according to the computational literature (Aiken, 1985; Miranker, 1981), even though there is debate regarding the true meaning of "stiff" problems (Aiken, 1985). Several numerical algorithm comparison studies have been conducted on "stiff" systems in order to determine which method(s) will provide reasonably accurate solutions at minimal computational cost(s) (Jackson and Sacks-Davis, 1980; Aiken, 1985; Bert and Stricklin, 1988). Common test problems have been confined to mass action kinetics or diffusion-convection problems. However, a multi-degree-of-freedom vibratory system with multiple clearances, used to model gear rattle type problems, is yet to be critically examined on a similar basis.

2 Scope and Objectives

This paper proposes a procedure for formulating the problem analytically before the governing equations are solved numerically. The process outlined is iterative in nature and it reduces some of the difficulties faced in vibro-impact system analyses. This procedure can be characterized as an "intelligent" pre-processing stage and is followed by the solution and/or the post-processing stage, where evaluation criteria are established for comparing various algorithms. Figure 1

Contributed by the Power Transmission and Gearing Committee for publication in the JOURNAL OF MECHANICAL DESIGN. Manuscript received Sept. 1992; revised Aug. 1994. Associate Technical Editor: D. R. Houser.

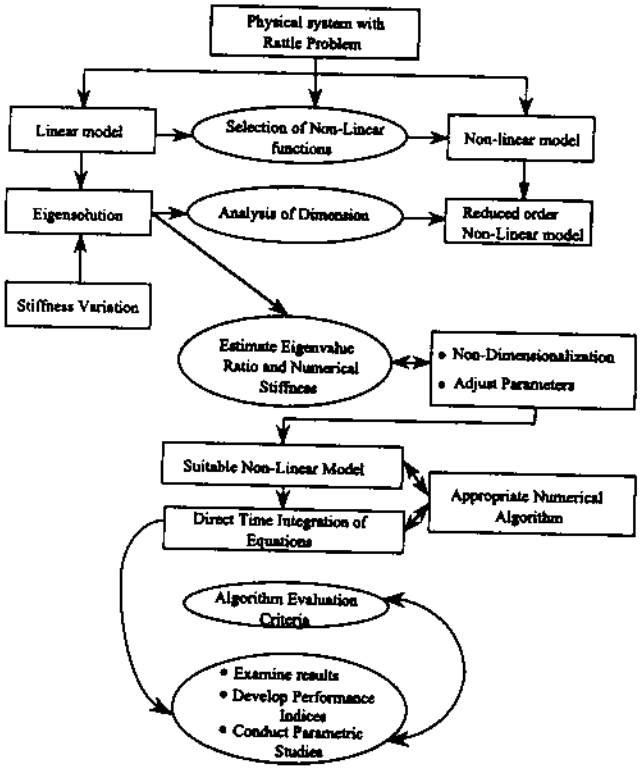

Fig. 1 The proposed procedure for solving rattle type problems

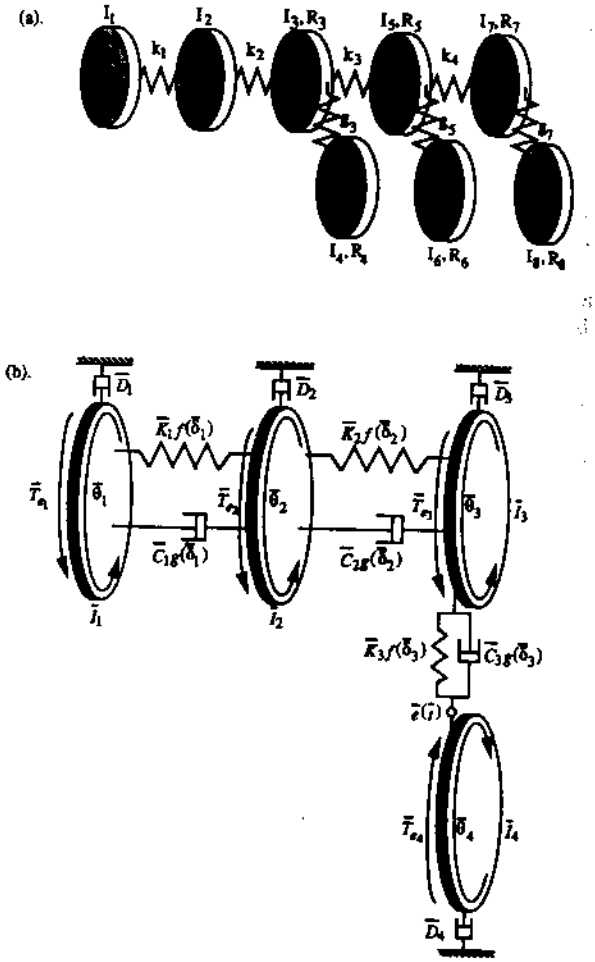

Fig. 2 Example cases: (a) eight-degree-of-freedom torsional model of an automotive transmission, and (b) generic four-degree-of-freedom geared system model with multiple clearance non-linearity, given by Eqs. (9) and (10).

shows a flowchart of the proposed problem solving procedure; it is based on our extensive experience with many simulations of gear rattle type problems. The first step is to examine the eigensolutions of the overall transmission system within the frequency range of interest. The nonlinear dynamic model can be linearized around an operating point and the corresponding linear model can be used to reduce the order or dimension of the model through appropriate lumping of various inertias. Next, a suitable non-linear model is developed and the governing equations of motion are written and then non-dimensionalized.

To understand the importance of "stiff" problems a linearized stiffness analysis based on the time-averaged gear mesh stiffness and/or clutch stiffness values is carried out. Such an analysis provides insight on the severity of the possible ill-conditioning which is then used to adjust the non-dimensionalizing parameters in order to reduce or avoid computational problems during the course of numerical integration. This is then followed by the selection of a suitable numerical algorithm to obtain actual solutions to the non-linear models and evaluating those solutions based on the criteria proposed. None of these issues have been addressed by prior gear rattle investigators.

3 Selection of System Dimension

As an example consider a hypothetical, yet reasonable, eight degree-of-freedom (DOF) torsional model of an automotive transmission with three gear pairs, a flywheel and a clutch as shown in Fig. 2(*a*). Initially all the torsional springs are assumed to be linear and the undamped system is solved for the natural frequencies ω_r and the corresponding mode-shapes or eigenvectors ψ_r ($r = 1, 2, \ldots, 8$). The ω_r values in rad/s are 0 (0), 346 (346), 7412 (7937), 10134, 18526, 48442 (48091), 50869, 68632; the values in parenthesis ( ) are the ω_r values of the reduced four DOF linear model of the same system, as shown in Fig. 2(*b*). The first two non-rigid body moves of the eight DOF model are given by $\psi_2 = [-0.01$ 0.98 1 1 1 1 1 $1]^T$ and $\psi_3 = [0$ 1 0 0 -0.3 -0.3 -0.5 $-0.5]^T$ respectively, where superscript T is the transpose. The excitation for such a system is usually of the form $T_e(t) = \Sigma_{j=1}^{n} T_{aj} \sin(j\Omega_e t)$ and is due to rotating mass unbalances and/or prime mover torque pulsations. The important excitation frequencies typically lie in the low frequency range, say 25–75 Hz. For this range of excitation frequencies the linear system response is dominated by the first mode (22 Hz) with a much smaller participation of the second mode. In each mode of vibration however, it is observed that there is little or no relative motion between the gear pairs. Based on this information one can then lump the second and third gears on the countershaft onto their conjugate parts on the mainshaft. Further one can lump the final two gears on the mainshaft onto the first gear, thus reducing the original eight degree-of-freedom, Fig. 2(*a*), system into a four degree-of-freedom model, Fig. 2(*b*). The inertia I_3 is replaced by $I_3 + I_5 + I_7 + I_6(R_5/R_6)^2 + I_8(R_7/R_8)^2$. At the end of this stage, the non-linear model can be developed.

4 Development of a Non-linear Model

The following non-linearities are introduced in the generic four degree-of-freedom model of Fig. 2(*b*): (*i*) a multi-staged clutch stiffness between the flywheel (I_1) and clutch (I_2) inertias, (*ii*) a clearance non-linearity between clutch (I_2) and input gear (I_3) inertias, and (*iii*) a backlash between the gears (I_3 and I_4). The governing equations of motion are as

follows

$$\bar{I}_1\ddot{\bar{\theta}}_1 + \bar{T}_{12} + \bar{T}_{d1} = \bar{T}_{e1}(t);$$

$$\bar{I}_2\ddot{\bar{\theta}}_2 - \bar{T}_{12} + \bar{T}_{23} + \bar{T}_{d2} = \bar{T}_{e2}(t) \quad (1, 2)$$

$$\bar{I}_3\ddot{\bar{\theta}}_3 - \bar{T}_{23} + \bar{R}_3\bar{F}_{34} + \bar{T}_{d3} = \bar{T}_{e3}(t);$$

$$\bar{I}_4\ddot{\bar{\theta}}_4 - \bar{R}_4\bar{F}_{34} + \bar{T}_{d4} = \bar{T}_{e4}(t) \quad (3, 4)$$

where $\bar{\theta}_i$, $\bar{I}_i$, $\bar{R}_i$, $(i = 1, \ldots, 4)$ are the torsional displacements, inertia values and radii of the inertia elements, respectively. The constraint torques $\bar{T}_{12}$, $\bar{T}_{23}$, force $\bar{F}_{34}$ and drag torques $\bar{T}_{di}$ are defined, in terms of the stiffness elements $\bar{K}_i$ and damping elements $\bar{C}_i$, as

$$\bar{T}_{12} = \bar{C}_1 g(\bar{\delta}_1)\dot{\bar{\delta}}_1 + \bar{K}_1 f(\bar{\delta}_1);$$

$$\bar{T}_{23} = \bar{C}_2 g(\bar{\delta}_2)\dot{\bar{\delta}}_2 + \bar{K}_2 f(\bar{\delta}_2) \quad (5, 6)$$

$$\bar{F}_{34} = \bar{C}_3 g(\bar{\delta}_3)\dot{\bar{\delta}}_3 + \bar{K}_3 f(\bar{\delta}_3); \quad \bar{T}_d = \bar{D}_{mi}\dot{\bar{\theta}}_{mi} + \bar{D}_{ai}\dot{\bar{\theta}}_{ai} \quad (7, 8)$$

where $\bar{\delta}_1 = \bar{\theta}_1 - \bar{\theta}_2$, $\bar{\delta}_2 = \bar{\theta}_2 - \bar{\theta}_3$, $\bar{\delta}_3 = \bar{R}_3\bar{\theta}_3 - \bar{R}_4\bar{\theta}_4 - \bar{e}(\bar{t})$ and $\bar{e}(\bar{t})$ is the transmission error. The excitation terms are given by $\bar{T}_{ei}(t) = \bar{T}_{mi} + \bar{T}_{ai}(t)$ with $\bar{T}_{ai}(t) = \sum_j \bar{T}_{a_{ij}} \sin(j\Omega_e t)$.

The *real life* clearance type non-linear elements, as shown in Fig. 2(*b*), can be related to the clutch torque characteristics or gear/spline backlash and are defined in terms of the following mathematical functions:

$$f(\bar{\delta}_i) = \begin{cases} \bar{\delta}_i - (1 - \alpha_i)\bar{b}_i, & \bar{b}_i < \bar{\delta}_i \\ \alpha_i\bar{\delta}_i, & -\bar{b}_i \le \bar{\delta}_i \le \bar{b}_i; \\ \bar{\delta}_i + (1 - \alpha_i)\bar{b}_i, & \bar{\delta}_i < -\bar{b}_i \end{cases}$$

$$g(\bar{\delta}_i) = \begin{cases} 1.0, & \bar{b}_i < \bar{\delta}_i \\ \beta_i, & -\bar{b}_i \le \bar{\delta}_i \le \bar{b}_i \\ 1.0, & \bar{\delta}_i < -\bar{b}_i \end{cases} \quad (9, 10)$$

5 Non-Dimensionalization

The equations of motion can be written in a non-dimensional form by defining $t = \bar{\omega}\bar{t}$, $\theta_i = \bar{\theta}_i/\bar{\psi}_c$, $\bar{\psi}_c = \bar{x}_c/\bar{R}_c$ where $\bar{\omega}$, $\bar{\psi}_c$, $\bar{x}_c$, $\bar{R}_c$ represent characteristic frequency, angular displacement, length and radius, respectively. The purpose of this procedure is two-fold. The first one is to reduce the number of system parameters and variables involved, and the second purpose is to possess a capability to adjust key parameters in such a manner which may effectively reduce the ill-conditioning of the system matrices during numerical integration. Ill-conditioning occurs due to the presence of components in the solution whose frequency ratio is large (Aiken, 1985; Hairer and Wanner, 1991). Then Eqs. (1–4) become

$$\theta_1'' + \eta_{11}g(\delta_1)\delta_1' + \Omega_{11}^2 f(\delta_1) - \xi_{11}\theta_1' = T_{e_1}(t) \quad (11)$$

$$\theta_2'' + \eta_{22}g(\delta_2)\delta_2' - \eta_{12}g(\delta_1)\delta_1' + \Omega_{22}^2 f(\delta_2) - \Omega_{12}^2 f(\delta_1) - \Omega_{12}^2 f(\delta_1) - \xi_{22}\theta_2' = T_{e_2}(t) \quad (12)$$

$$\theta_3'' + \eta_{33}g(\delta_3)\delta_3' - \eta_{23}g(\delta_2)\delta_2' + \Omega_{33}^2 f(\delta_3) - \Omega_{23}^2 f(\delta_2) - \xi_{33}\theta_3' = T_{e_3}(t) \quad (13)$$

$$\theta_4'' - \eta_{34}g(\delta_3)\delta_3' - \Omega_{34}^2 f(\delta_3) - \xi_{44}\theta_4' = T_{e_4}(t) \quad (14)$$

Here the prime denotes differentiation with respect to t and individual terms are defined below:

$$\xi_{ii} = \frac{\bar{D}_i}{\bar{I}_i\bar{\omega}}; \quad \eta_{ij} = \frac{\bar{C}_i}{\bar{I}_j\bar{\omega}}, \quad i = 1, 2; \quad j = 1, 2, 3;$$

$$\eta_{3k} = \frac{\bar{R}_c\bar{R}_k\bar{C}_3}{\bar{I}_k\bar{\omega}}, \quad k = 3, 4 \quad (15\text{–}17)$$

$$\Omega_{ij}^2 = \frac{\bar{K}_i}{\bar{I}_j\bar{\omega}^2}, \quad i = 1, 2; \quad j = 1, 2, 3;$$

$$\Omega_{3k}^2 = \frac{\bar{R}_c\bar{R}_k\bar{K}_3}{\bar{I}_k\bar{\omega}^2}, \quad k = 3, 4 \quad (18, 19)$$

$$T_{e_i}(t) = \frac{\bar{T}_{m_i} + \bar{T}_{a_i}(t)}{\bar{I}_i\bar{\omega}^2\bar{\psi}_c}, \quad \bar{T}_{a_i}(t) = \sum_j \bar{T}_{a_{ij}} \sin(\Omega_{e_{ij}}t);$$

$$e(t) = \epsilon \sin\left(N\Omega_{e_{11}}t\right) \quad (20\text{–}22)$$

where $\Omega_{e_{ij}} = j\bar{\Omega}_{e_i}/\bar{\omega}$, $i = 1, \ldots, 4$ and $j = 1, 2, \ldots$ and N is the number of gear teeth.

6 Numerical Stiffness Issue

The equations developed in section 5 can be written in vector form as $d\mathbf{y}/dt = \mathbf{p}(\mathbf{y}, t)$. Most numerical codes linearize around an operating point $\mathbf{y}_0$, hence we have the following expression where the higher order terms are ignored: $\mathbf{p}(\mathbf{y}, t) \cong \mathbf{p}(\mathbf{y}_0, t) + \mathbf{J}(\mathbf{y} - \mathbf{y}_0)$, where $\mathbf{J} = d\mathbf{p}/d\mathbf{y}|_{\mathbf{y}_0}$ is the Jacobian matrix. The local eigenvalues of the Jacobian is used to define numerical "stiffness." Aiken (1985) classifies the vibro-impact problem as *stubborn* due to system discontinuities, re-occurring mechanical or physical stiffness and the possibility of the existence of highly oscillatory components. He defines numerical stiff categories based on $\mathbf{R}_\lambda$, the ratio of the largest eigenvalue (in magnitude) to the smallest non-zero eigenvalue: (*i*) Mildly stiff: $\mathbf{R}_\lambda < 10^2$; (*ii*) Strongly stiff: $10^3 < \mathbf{R}_\lambda < 10^5$, (*iii*) Extremely stiff: $10^6 < \mathbf{R}_\lambda < 10^8$, and (*iv*) *Pathologically* stiff: $10^9 < \mathbf{R}_\lambda$. Also, Hairer and Wanner (1991) evaluate numerical stiffness in terms of the magnitude of the largest eigenvalue. According to them numerical stiffness occurs when the product of the dominant eigenvalue and the step size lies on the border of the stability domain of the numerical algorithm.

In order to estimate $\mathbf{R}_\lambda$ and/or the largest eigenvalue, a new concept of stiffness contact ratio Γ is introduced here; *it should not be confused with the classical contact ratio of gears.* The idea behind this procedure is to replace the time dependent Jacobian components (essentially the non-linear elements) by a time-averaged value. When such a linearization is done the eigenvalues of the Jacobian correspond to the eigenvalues of the physical model itself. This is explained by using the gear pair as an example. If two gears are connected by a backlash element the pair may become physically uncoupled. A loss of contact can be due to an alternating load, light mean load and/or a combination of both. Hence, a linear effective stiffness based on the time the pair is uncoupled can be defined. The fraction of the time the pair is uncoupled defines Γ_g. For instance if the gears are in the backlash region 50 percent of the time then $\Gamma_g = 0.5$. One can obviously assume a specific value. However Γ is not necessarily equal to $0.50(1 + \alpha)$, but may be estimated by using nonlinear analyses in one of the following ways:

(*I*) By using the cross and auto power spectral densities to estimate the linearized transfer function from which the dynamic stiffness may be obtained. See Bendat and Piersol (1986) for typical signal processing issues.

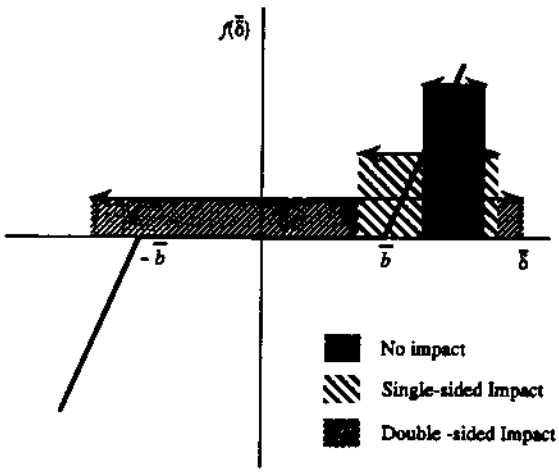

Fig. 3 Three different vibro-impact regimes for a backlash type of non-linearity given by Eq. (9) with $\alpha_i = 0$

(2) By keeping track of the time history of $df(\delta)/d\delta$ which is a square wave bounded between zero and one; it may not be periodic depending on the nature of the response. Then Γ may be found by time averaging the signal *i.e.*, $\Gamma = 1/N\{\Sigma_{m=1}^{N}[df(\delta)/d\delta]_{t_m}\}$ and is between 0 and 1.

(3) By using the describing function or harmonic balance method (Gelb and Vander Velde, 1968; Comparin and Singh, 1989) to analytically approximate the value of Γ. This method has the benefit that if one has a prior knowledge of the expected amplitude of motion, the stiffness contact ratio can be obtained without any numerical simulations. Figure 3 shows the three types of impacts possible, and Fig. 4 shows typical Γ_g values for the single-sided and double-sided impact cases. As can be seen from these results, an increase in the amplitude of single-sided impacts means more time is being spent in the backlash region thus reducing Γ_g. For the double-sided case, a very large amplitude results in a saturation effect pushing Γ_g towards one.

7 Results Using Stiffness Contact Ratio Γ

The concept of stiffness contact ratio, Γ, is now used in the four degree-of-freedom model developed earlier and the function $f(\delta_1)$ is replaced by $\Gamma_c\delta_1$ and the function $f(\delta_3)$ is replaced by $\Gamma_g\delta_1$, where $0 < \Gamma_c < 1$ and $0 < \Gamma_g < 1$ [in Eqs. (1)–(4) and (11)–(14)]. Here $f(\delta_2)$ is assumed to be δ_2 (linear) and the modified system's natural frequencies (undamped) are evaluated. Equations (1)–(4) and (11)–(14) have all the variables in the torsional form. One could instead consider a mixed form, for instance, replacing θ_3 by $x_3 = R_3\theta_3$, and θ_4 by $x_4 = R_4\theta_4$. This form has two torsional variables and two translational variables. The mixed formulation (non-dimensional) is effective in reducing ill-conditioning when compared to a pure torsional or translational formulation. In fact the pure torsional or translational non-dimensional formulation gives the same R_λ as the corresponding dimensional formulation. Hence all the subsequent results use a mixed formulation. Figure 5 shows a plot of the three non-rigid body frequencies as Γ_g is varied for $\Gamma_c = 0.10$ while Fig. 6 illustrates a variation in $\mathbf{R}_\lambda$ as Γ_g is varied. It is observed from these results that the stiffness ratio is indeed lower for the non-dimensional case. Actual numerical integrations (though not included here) confirm these trends. This demonstrates the effectiveness of the non-dimensional formulation in reducing or avoiding ill-conditioning. This is clearly seen from Fig. 6(*b*) where in the dimensional case the highest $\mathbf{R}_\lambda$ value is about seventy five; conversely the maximum non-dimensional value barely crosses twenty. This definitely improves the computational efficiency. The study also

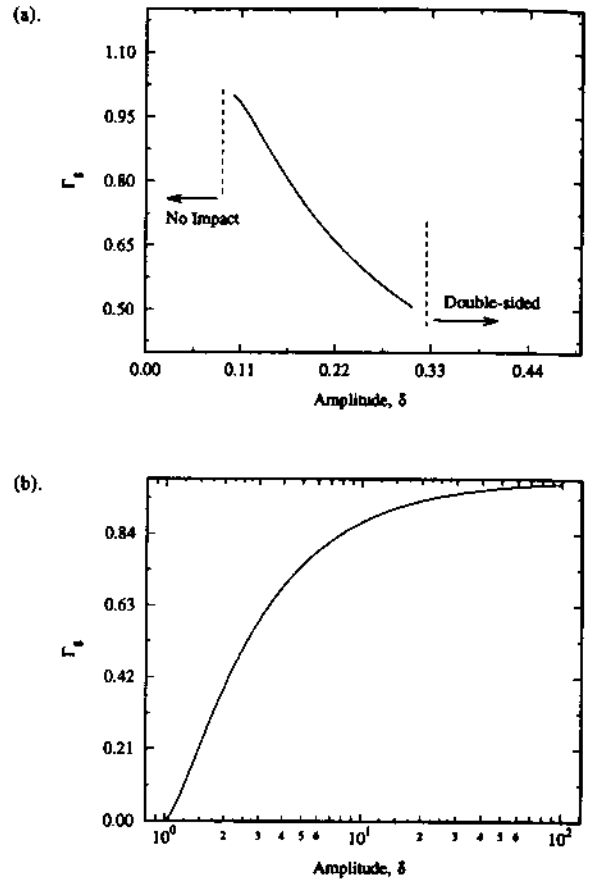

Fig. 4 The variation of Γ_g with the response amplitude δ, for (a) single-sided impacts, and (b) double-sided impacts

shows that at low stiffness contact ratios (associated with light mean loads and/or high alternating loads) the natural frequencies are much closer than at high stiffness contact ratios. Based on these results strong nonlinear behavior is anticipated at low loads, which is confirmed by actual time integration.

8 Example Cases and Algorithm Evaluation Criteria

An analysis of numerical methods will be conducted using parameters from a generic automotive manual transmission (See Fig. 2). Baseline inertial and stiffness parameters are incorporated into the dimensionless format [refer to Eqs. (11)–(14)] and these are listed in Table 1. Typical values used to define the non-linearities will be given later. Three example cases of differing complexity, from moderately non-linear (case 1) to extremely non-linear (case 3), are listed in Table 2. The extent of the stiffness non-linearity for each element is categorized as moderately non-linear (i.e. $\alpha < 0.01$) and strongly non-linear ($\alpha < 0.01$). Since damping element non-linearities are associated with the stiffness changes, clearance non-linearities increase or decrease modal damping.

The algorithms considered for this study are the Runge-Kutta fixed step second and fourth order (RK2, RK4), variable step size Runge-Kutta-Fehlberg (4th order integrator and 5th order error estimator; RKF) and Runge-Kutta-Verner (5th order integrator and 6th order error estimator, RKV), Adams variable step and order (ADM; IMSL, 1986), Gear's stiff (GRS; Hindmarsh, 1974), and the Bulirsch-Stoer (BUS) methods.

The numerical indices which may be used to evaluate an algorithm are: (*i*) computational performance indices for a given algorithm, and (*ii*) indices used to compare the solu-

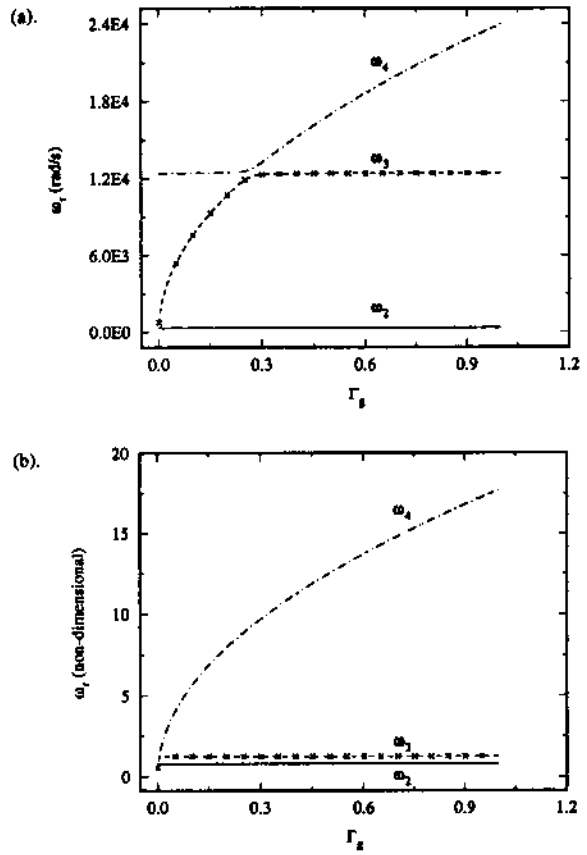

Fig. 5 The changes in ω_r of the four-degree-of-freedom system, shown in Fig. 2(*b*) for $\Gamma_c = 0.10$; (*a*) dimensional case, and (*b*) non-dimensional case

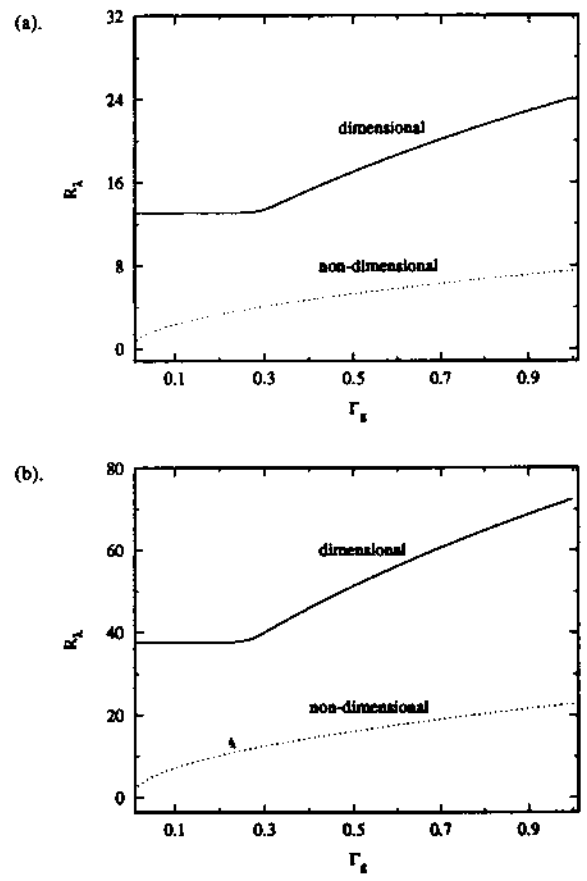

Fig. 6 Variation of R_A with Γ_g for (*a*) $\Gamma_c = 1.0$, and (*b*) $\Gamma_c = 0.10$

Table 1 Dimensionless parameters for numerical study†

ξ_{11}	ξ_{22}	ξ_{33}	ξ_{44}
3.333e-06	0.002	9.524e-05	1.667e-04
η_{11}	η_{12}		η_{22}
0.005	3.333		0.111
η_{23}	η_{33}		η_{34}
0.005	7.143		50.000
Ω_{11}^2	Ω_{12}^2		Ω_{22}^2
0.222	148.148		1482.0
Ω_{23}^2	Ω_{33}^2		Ω_{34}^2
63.49	7619.0		5.333e04

Table 2 Some case study models†

Case	Element Features	Index i	α_i	β_i	δ_i	Comments
1	m NL	1	0.10	0.25	160.0	two nonlinear oscillators connected by a linear oscillator
	linear	2	1.0	1.0	∞	
	backlash	3	0.0	0.0	1.0	
2	m NL	1	0.01	0.025	160.0	three nonlinear oscillators (includes transmission error excitation)
	backlash	2	0.0	0.0	58.67	
	backlash	3	0.0	0.0	1.0*	
3	s NL	1	0.001	0.01	160.0	three nonlinear oscillators severe coupling possible
	backlash	2	0.0	0.0	58.67	
	backlash	3	0.0	0.0	1.0*	

* Transmission error amplitude 0.1; m NL: moderately nonlinear; s NL: strongly nonlinear

† Refer to Figure 2 and the text for identification of the variables.

tions provided by different algorithms for the same physical problem. In the first category the commonly used criteria are the following:

(*a*) *Total time required for the solution*: This may represent a useful comparison from a users viewpoint since an excessive computational time may slow down research.

(*b*) *Number of steps and function calls*: These two indices are closely tied to the total time. However, an unusually high number of steps or function calls may be an indicator of an algorithm having difficulty obtaining solutions near critical points, say at the physical discontinuity of the system model.

(*c*) *Tolerance*: This is a user defined parameter to ensure a certain accuracy of solution. Each algorithm attempts to control the norm of the local error so that the error is proportional to the tolerance. Obviously, a solution with a high tolerance value requires a smaller h and longer computational times than that with a low tolerance.

For the second category four main criteria have been developed to compare the solutions provided by the different algorithms for the gear rattle type problems:

(*a*) *Time domain results*: Time history output is conveniently placed in the form of a graph with abscissa-normalized time to reflect cycles of fundamental period corresponding to the excitation frequency. Thus super- or sub-harmonic responses are easily ascertained.

(*b*) *Transmissibility* TR: This is a numerical measure of the agreement between time domain solutions and is defined as follows:

$$TR_{rms} = \frac{\theta''_{4_{rms}}}{\theta''_{1_{rms}}}; \quad \theta_{i_{rms}} = \left[\frac{1}{T}\int_0^T (\theta_i'')^2 dt\right]^{1/2}, \quad i = 1, 4;$$

$$TR_{peak} = \frac{\theta''_{4_{peak}}}{\theta''_{1_{peak}}} \quad (23\text{–}25)$$

where the subscript peak refers to the peak to peak value of the acceleration over the period of interest. This index is applied only to the steady state time domain solutions with

rms and peak TR values computed from a span of eight cycles.

(*c*) *Spectral Contents*: The frequency spectrum enables quick identification of primary response frequencies.

(*d*) *Solution coherence* $\kappa_{xy}(f)$: Since vibro-impacts induce broadband frequency response, one finds difficulty in the comparison of frequency domain information. Hence, in order to determine the agreement of the solutions, only selected frequencies or bandwidths were used in the determination of $\kappa_{xy}(f)$, which is defined as $|(P_{xy}(f))^2|/P_{xx}(f)P_{yy}(f)$ where $P_{xx}(f)$, $P_{yy}(f)$ and $P_{xy}(f)$ are the averaged auto, auto and cross power spectral densities (PSD), respectively. Typical signal processing includes 128 points per time window and four ensembles. The RK2 time domain results were used as a reference for comparison.

9 Results and Validation of Models

Three selected case studies as identified in Table 2 are presented, covering a range of complexity regarding the number of non-linear elements and types of loading; also refer to Fig. 2. The typical excitation in each case consists of a mean load and five harmonics of sinusoidal load applied to the inertial element I_1, a mean load applied to I_4, and light drag loads applied to all elements. Additionally, cases 2 and 3 include transmission error excitation applied at the mesh frequency $20\Omega_{e_{11}}$ where $\Omega_{e_{11}}$ is the frequency of the main shaft rotation.

Tables 3 and 4 show performance criteria for a system with two and three clearance type non-linearities with multiple excitations (case 1 and case 3, respectively). Note from the tables that the computational time increases as the number of non-linearities increase, as expected. The increased times of RK2 and RK4 are half that of the variable step routines, while still maintaining compatible solutions. This is because the variable step method hunts for an optimal time integrating step h thus leading to extra time. Since the RK2 method is similar to the Euler method it performs better in dealing with eigenvalues which are highly oscillatory.

Higher order methods may become locally unstable for similar eigenvalues, necessitating stepsize adjustments. The variable stepping methods generally show a larger initial average trial step size $\hat{h}_i$, but it is noted that this trial size nearly always fails near the breakpoints of the physical non-linear functions. The step size reductions that ensue require much code and repetition, thus increasing the computing

Table 3 Algorithm computational performance indices for case 1

Algorithm	Average step $\hat{h}_i$	Number of steps	Number of function calls	Run time min:sec
RK2	0.001	800000	1600000	25:47
RK4	0.0128	64000	256000	17:02
RKF	0.0058	142034	846206	27:37
RKV	0.0074	116533	1185328	28:20
GRS	0.0040	315600	462100	16:29
ADM	0.0039	301000	427400	24:45
BUS	0.0145	51607	1152692	22:15

Table 4 Algorithm computational performance indices for case 3 $\epsilon = 0.10$

Algorithm	Average step $\hat{h}_i$	Number of steps	Number of function calls	Run time min:sec
RK2	0.001	850000	1700000	28:08
RK4	0.0128	67000	268000	18:44
RKF	0.0400	125034	1150312	33:24
RKV	0.0377	170441	2090359	50:03
GRS	0.0404	246600	921000	19:55
ADM	0.0365	411500	678400	33:59
BUS	*****	*****	*****	*****

*****: Failed to converge

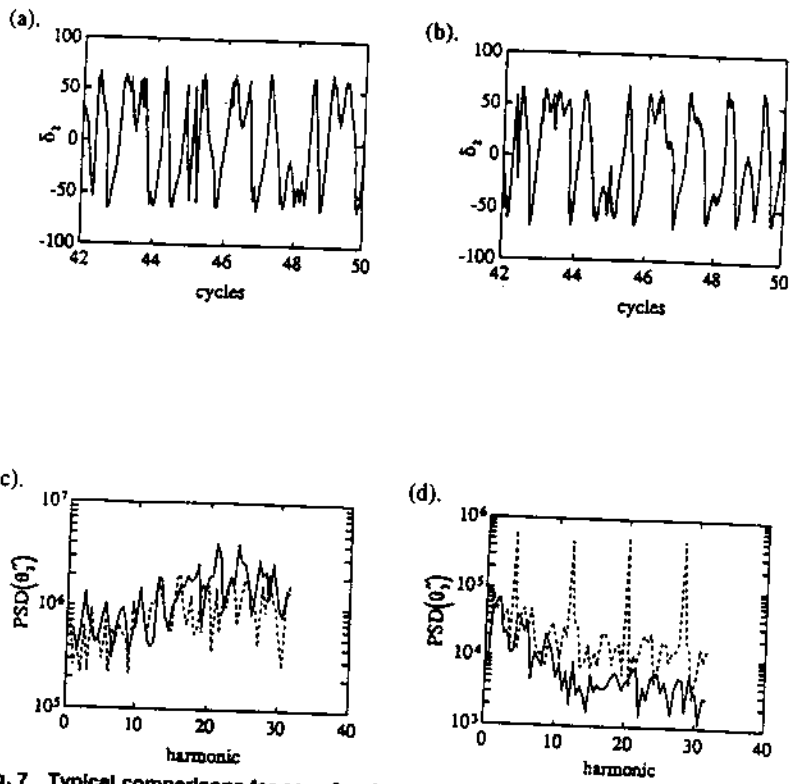

Fig. 7 Typical comparisons for case 3: relative displacements in time domain using (*a*) second order Runge-Kutta algorithm (RK2) (*b*) Runge-Kutta-Verner algorithm (RKV), (*c*) and (*d*). Power spectral densities with $\epsilon = 0.10$; — second order Runge-Kutta method (RK2) and ___ Gear stiff method (GRS)

Table 5 Comparison between simulation and experiment for the system shown in Fig. 2(b)

Case	Peak to Peak torsional acceleration (rad/s²)					
	$\ddot{\delta}_1$			$\ddot{\delta}_3$		
Type	Experiment	Simulation	σ %	Experiment	Simulation	σ %
1	1052	983	6.56	1510	1540	-1.95
2	1481	1260	14.9	2090	1862	10.9
3	2094	1963	6.26	2168	2247	-3.64

σ = 100(Experiment -Simulation)/Experiment

time. Note that for case 3 when $e(t)$ is the dominant excitation, the Bulirsch-Stoer (BUS) method fails to converge. This was the only routine, of all seven tested, that consistently displayed convergence failures and incompatible solutions, especially for systems with multiple non-linearities.

Figures 7(*a*) and 7(*b*) show a typical comparison of the time domain solutions yielded by RK2 and RKV for case 3. One can notice slight variations between the two solutions. Figures 7(*c*) and 7(*d*) compare spectra between RK2 and GRS schemes for case 3. The GRS algorithm has a tendency to smooth out the high frequency components. The coherence factors (based on first five harmonics) of the absolute accelerations for case 2 are given by $\kappa_{\theta_i'',\theta_{iref}''} = 0.76$, 0.23, 0.53 and 0.37 for the RK4 scheme; $\kappa_{\theta_i'',\theta_{iref}''} = 0.9$, 0.23, 0.58 and 0.35 for the RKV method; $\kappa_{\theta_i'',\theta_{iref}''} = 0.79$, 0.41, 0.54 and 0.59 for the GRS numerical scheme. Here i varies from 1 to 4 and the reference numerical scheme is RK2. Observe that these values degrade for the solutions far away from the driving point of either the torque or transmission error excitation. Note that it is more difficult to find the solution at I_2 than at other inertial points. This could be attributed to the relationship between stiffnesses and mass loading effect upon I_2, combined with the stabilizing effect of the mean load on I_4. Also the TR yielded by the fixed step routines appear to encompass a larger bandwidth (rms to peak) than those yielded by higher order algorithms. This may be due to the inherent smoothening effect higher order methods impose.

Loading effects are also examined. For case 3, the ratio of the mean to alternating load is set to 0.05 for the lightly loaded case and 0.5 for the moderately loaded case. An increase in the mean load on the system reduces the computing time for variable step algorithms by about 30 percent. The solution coherences are also better for such moderately loaded systems.

In order to validate the proposed numerical techniques for non-linear systems, results were compared with available experimental data (Takemoto et al., 1992) from a four-degree-of-freedom system, as shown in Fig. 2(*b*). Comparisons between simulation and experimental angular accelerations (in rad/s²) are found to be excellent for three different cases, as evident from Table 5. These results and other comparisons (though not reported here because of industrial proprietary information involved) are very promising and indicate that the techniques presented in this study are indeed suitable.

The choice of an algorithm is dictated by the type of physical system, including nonlinearities, under evaluation. For instance, higher order methods appear to become computationally inefficient as evident from the excessive computational time and functional calls when the system becomes one or any combination of the following: lightly loaded, lightly damped, highly non-linear, or strongly stiff. Such computational inefficiency does not necessarily mean that the solutions obtained are inconsistent with other data, only that the lower order fixed step methods operate faster than the higher order variable steppers. Numerical *stiffness* becomes an issue for all algorithms tested since a system with clearance type non-linearities has the potential to become strongly stiff, forcing numerical integration schemes to severely restrict step size. A variable step or variable order algorithm typically senses the physical discontinuity and in the attempt to step across it, "bottoms out," reducing h to the prescribed user tolerance. Conversely the fixed step methods tend to walk through the discontinuities and have the ability to converge quickly after the step, in most cases (see case 3). This appears to be one of the main reasons why fixed stepping routines ran faster in nearly every case. This feature has been noted in the literature and new integration algorithms incorporating order reduction, when discontinuities are evident, have begun to appear (Chi and Tucker, 1982; Cash and Karp, 1990).

10 Concluding Remarks

The entire problem formulation and pre-processing process described in this paper is iterative in nature and discretion or caution must be exercised by the analyst at each stage. It must be completed in order to generate a suitable set of non-linear ordinary differential equations. This procedure is used to detect trends which could cause significant numerical problems or changes in dynamic response. At the end of this process a suitable algorithm must be selected by the user which is then utilized to carry out simulation and parametric design studies of the system. The evaluation of numerical integration methods, as presented here, for clearance-type non-linear geared torsional systems is believed to be the first of its kind. It has been shown that the evaluation of clearance-type torsional systems rely critically on the choice of an algorithm, and some of the pitfalls encountered have been documented. However it is still a limited study and therefore any conclusions derived here must be considered as preliminary since only seven different algorithms have been evaluated. Further research, which addresses several of the unresolved issues, is in progress.

Acknowledgment

We wish to acknowledge the Nissan Technical Center (Japan) and the Center for Automotive Research at the Ohio State University for supporting this research.

References

Aiken, R. C., 1985, "Classification of Other 'Stubborn' Problem Types," *Stiff Computation*, Aiken, R. C., ed., Oxford University Press, New York, pp. 16–21.

Bendat, J. S., and Piersol, A. G., 1986, *Random Data: Analysis and Measurement Procedures*, Second edition, John Wiley and Sons, New York.

Bert, C. W., and Stricklin, J. D., 1988, "Comparative Evaluation of Six Different Numerical Integration Methods for Non-linear Dynamic Systems," *Journal of Sound and Vibration*, Vol. 127, pp. 221–229.

Cash, J. R., and Karp, A. H., 1990, "A Variable Order Runge-Kutta Method for Initial Value Problems with Rapidly Varying Right-hand Sides," ACM *Transactions on Mathematical Software*, Vol. 16, No. 3, pp. 201–222.

Chi, M., and Tucker, J., 1982, "Integration Methods for Stiff Systems," *Structural Mechanics Software Series*, Perrone, N., and Pilkey, W., eds., Vol. IV, University Press of Virginia, Charlottesville.

Chikatani, Y., and Suehiro, A., 1991, "Reduction of Idling Rattle Noise in Trucks," SAE Paper No. 911044, pp. 49–56.

Comparin, R. J., and Singh, R., 1989, "Frequency Response Characteristics of an Impact Pair," *Journal of Sound and Vibration*, Vol. 134, pp. 259–290.

Comparin, R. J., and Singh, R., 1990, "Frequency Response of Multi-Degree-of-Freedom Systems with Clearances," *Journal of Sound and Vibration*, Vol. 142, pp. 101–124.

Croker, M. D., March, J. P., and Greer, R. J., 1990, "Transmission Rattle Analysis," *Proceedings of IMechE, First International Conference on Gearbox Noise and Vibration*, C404/005, pp. 121–127.

Gaffney, P. W., 1984, "A Performance Evaluation of Some FORTRAN Subroutines for the Solution of Stiff Oscillatory Ordinary Differential

Equations," ACM *Transactions on Mathematical Software*, Vol. 10, No. 1, pp. 58–72.

Gelb, A., and Vander Velde, W. E., 1968, *Multiple-Input Describing Functions and Nonlinear System Design*, McGraw-Hill, New York.

Hairer, E., and Wanner, G., 1991, *Solving Ordinary Differential Equations II: Stiff and Differential-Algebraic Problems*, Springer-Verlag, Berlin.

Hindmarsh, A. C., 1974, "GEAR: Ordinary Differential Equation System Solver," Lawrence Livermore Laboratory Report UCID-30001, Revision 3.

IMSL, 1986, *User's Manual*, edition 1.0, IMSL, Houston.

Jackson, K. R., and Sacks-Davis, R., 1980, "An Alternative Implementation of Variable Multi-step Formulas for Stiff ODEs," ACM *Transactions on Mathematical Software*, Vol. 6, No. 3, pp. 295–318.

Johnson, O., and Hirami, N., 1991, "Diagnosis and Objective Evaluation of Gear Rattle," SAE Paper No. 911082, pp. 381–396.

Miranker, W. L., 1981, *Numerical Methods for Stiff Equations and Singular Perturbation Problems*, D. Reidel Publishing Company, Boston.

Pfeiffer, F., and Kunert, A., 1990, "Rattling Models from Deterministic to Stochastic Processes," *Nonlinear Dynamics*, Vol. 1, pp. 63–74.

Sakai, T., Doi, Y., Yamamoto, K., Ogasawara, T., and Narita, M., 1981, "Theoretical and Experimental Analysis of Rattling Noise of Automotive Gearbox," SAE Paper No. 810773, pp. 1–10.

Seaman, R. L., Johnson, C. E., and Hamilton, R. F., 1984, "Component Inertial Effects on Transmission Design," SAE Paper No. 841686, pp. 1–19.

Singh, R., Xie, H., and Comparin, R. J., 1989, "Analysis of Automotive Neutral Gear Rattle," *Journal of Sound and Vibration*, Vol. 131, pp. 177–196.

Takemoto, K., Yokoyama, Y., and Abe, T., 1992, Personal Communication, Nissan Technical Center.

Veluswami, M. A., and Crossley, F. R. E., 1975, "Multiple Impacts of a Ball between Two Plates, Part 1: Some Experimental Observations," ASME *Journal of Engineering for Industry*, Vol. 19, pp. 820–827.